Advances in Aerospace Science and Technology, 2022, 7, 112-122
https://www.scirp.org/journal/aast
ISSN Online: 2473-6724
ISSN Print: 2473-6708

Calculation of Aerodynamic Characteristics of Hypersonic Vehicles Based on the Surface Element Method

Tianqiang Huang, Guoyi He, Qi Wang

Nanchang Hangkong University, Nanchang, China
Email: hegy509@163.com, huang002320@163.com

How to cite this paper: Huang, T.Q., He, G.Y. and Wang, Q. (2022) Calculation of Aerodynamic Characteristics of Hypersonic Vehicles Based on the Surface Element Method. *Advances in Aerospace Science and Technology*, **7**, 112-122.
https://doi.org/10.4236/aast.2022.72007

Received: March 30, 2022
Accepted: May 24, 2022
Published: May 27, 2022

Abstract

A program for calculating the aerodynamic properties of hypersonic vehicles based on the surface element method was developed using the general-purpose programming language C++. The calculated values of lift coefficients, drag coefficients, and surface pressure coefficients are discussed with the results of wind tunnel experiments using the HL-20 lift body and the NASA hypersonic aircraft STS Columbia OV-102 as research subjects. Finally, the results of the experimental and wind tunnel studies of the aerodynamic characteristics of the HL-20 lift body at an altitude of 65 km and Mach numbers of 6 and 10 Ma are discussed. The maximum error in the aerodynamic characteristics at 6 Ma does not exceed 3%, consistent with the results. The maximum error at 10 Ma occurs in the 11˚ - 14˚ angle of attack and does not exceed 10%, which is still within the error tolerance. The STS results for NASA's hypersonic aircraft were also tested using this procedure. Experimental aerodynamic data for the Colombian OV-102 aircraft. The results show that the program takes only 10 minutes to calculate the results, with no more than 2% error from the wind tunnel experimental results.

Keywords

Surface Element Method, Hypersonic Vehicle, C++, Aerodynamic Characteristics, Engineering Calculations

1. Introduction

Hypersonic vehicles are receiving worldwide attention. Their design and development require an in-depth understanding of hypersonic flows. Accurate prediction of hypersonic flow around re-entry vehicles remains one of the most challenging problems in aerospace engineering. The aerodynamic properties of hypersonic vehicles are a prerequisite for determining their aerodynamic shape, flight trajectory, and flight performance. The pressure and surface sassafras distribution, closely related to aerodynamics, is critical for deciding hypersonic vehicles' loading conditions and thermal environment. Irimpan, K. *et al.* addressed the problem of nose tip transition control of surface roughness of hypersonic spheres [1]. In 2021, Li Jin *et al.* compared the effect of the hypersonic vehicle from continuous to free molecular flow on aerodynamic properties using direct simulation Monte Carlo and unified gas dynamics schemes [2]. A finite element method based on supermodel theory to calculate the coupling coefficients of a twin-core fiber was proposed by Zhao Tianhao *et al.* [3]. The conventional CFD method is limited by the long simulation time and economic conditions, and the current wind tunnel cannot fully simulate the hypersonic flight environment of the vehicle. In this paper, for the complex aerodynamic layout of the flying wing re-entry vehicle, a fast aerodynamic calculation procedure for the flying wing re-entry vehicle is developed independently based on the integration of existing engineering calculation methods to calculate the NASA hypersonic aircraft STS Columbia OV-102 at Mach 8 flight speed, 30˚ angle of attack based on the streamline tracing technique, and the surface Pressure coefficients were calculated for the HL-20 horizontal landing spacecraft at different Mach numbers and angles of attack using this method. In this paper, the results of wind tunnel tests [4] are compared and analyzed to verify the timeliness and accuracy of the method. The aerodynamic characteristic coefficients calculated by this procedure combined with the Kemp-Riddell heat flow formulation can also be used to study hypersonic heat flow variations. In 2022 Yang Z *et al.* discussed the effect of wall temperature variation on hypersonic vehicle boundary layer heat flow [5].

2. Computational Programming

The hypersonic vehicle aerodynamic engineering calculation program developed in this paper consists of four parts: the open-source program NETGEN [6] [7] for mesh division reading, correction of the average vector of the surface element, and aerodynamic calculation, and result output. Integrating each module allows the engineering calculation of hypersonic vehicle aerodynamics to be realized quickly. The correction is performed according to the method proposed by Zhengzhou Li [8] for immediate modification of the out-of-grid average vector. In this paper, we use the alternating digital tree data structure (ADT) to manage all the HL-20 divided surface elements and then use the ray projection algorithm to correct the average vector by judging the parity number of ray intersection with the surface elements [9].

2.1. Calculation of Aerodynamic Coefficient

As in **Figure 1**, by solving the geometric relationship of the velocity vector of the

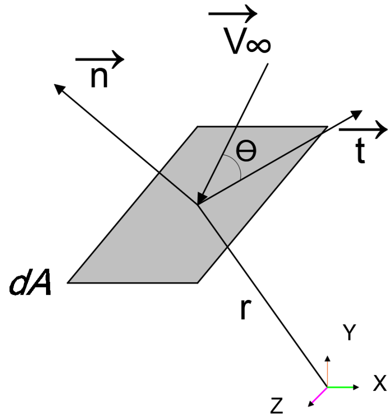

Figure 1. Schematic diagram of the impact angle.

surface element coordinate system. It is then possible to calculate the angle of impact of the free incoming flow with the vehicle's surface. The velocity vector of the free incoming flow is input through the interaction window, and the normal vector of the surface element is calculated with the correction completed in the previous subsection by Equation (1) to calculate the magnitude of the impact angle.

$$\theta = \frac{\pi}{2} - \cos^{-1}\frac{\boldsymbol{N}\cdot\boldsymbol{V}}{|\boldsymbol{N}||\boldsymbol{V}|} \tag{1}$$

Taking values in the range [−π/2, π/2].

Different empirical formulas need to be used for the windward and leeward surfaces in the engineering calculations of aerodynamic engineering properties. For the classical Newtonian theory to calculate the vehicle's aerodynamic properties, it is assumed that there is no collision between the fluid and the leeward surface, considering $C_p = 0$. The pressure coefficient of each surface element is directly related to the magnitude of the aerodynamic force on that surface element. The procedure designed in this paper chooses the Dahlem-Buck formula for calculating the windward surface based on the Newtonian method and the tangent cone method [10]. The pressure coefficient of the leeward surface is computed using the ACM empirical formula.

1) Dahlem-Buck formula

$$C_p = C_{pD}\cdot\frac{C_{pcone}\left(Ma_\infty \le 20\right)}{C_{pcone}\left(Ma_\infty = 20\right)} \tag{2}$$

$$C_{pD} = \begin{cases}\left[\dfrac{1}{\sin^{3/4}\left(4\theta\right)}+1\right]\sin^2\theta, & 0\le\theta\le 22.5^\circ \\ K\sin^2\theta, & \theta\ge 22.5^\circ\end{cases} \tag{3}$$

By fitting a large amount of experimental data, the values taken in the Dahlem-Barker formula can be calculated with different fitting formulas according to the vehicle's various parts.

For the fuselage:

$$K = 2.38 + 0.03792\theta - 0.002521\theta^2 + 0.000045830\theta^3 + 2.917\times10^{-7}\theta^4 \tag{4}$$

For the wings:

$$K = 3.24 - 0.08867\theta + 0.002775\theta^2 - 4.333\times10^{-5}\theta^3 + 2.5\times10^{-7}\theta^4 \tag{5}$$

For operating the helm surface:

$$K = 1.15 + 0.0041179\theta + 0.0009958\theta^2 - 4.166\times10^{-6}\theta^3 + 4.166\times10^{-8}\theta^4 \tag{6}$$

2) ACM Experience formula

$$C_p = \max\left[-\left(\frac{\theta}{15}\right)\left(\frac{1}{Ma^2}\right)-\left(\frac{1}{Ma^2}\right)\right] \tag{7}$$

The program uses the two methods mentioned above to calculate the surface pressure coefficient for each surface element and stores the calculation results in the.dat folder.

2.2. Output of Calculation Results

The coupling effects of the viscous-free aerodynamic properties under hypersonic conditions are minor. The axial force, normal force, lateral force, and moment coefficients on each surface element can be obtained. Summing these coefficients, the whole model's total aerodynamic force and moment coefficients can be obtained. The modeled body coordinate system performs the calculation of the surface element aerodynamic forces and moments. In order to get the total aerodynamic forces and moment coefficients, they need to be converted to the body and velocity coordinate systems for processing.

$$C_x = \sum\frac{C_p n_x \Delta A}{S_{ref}} \tag{8}$$

$$C_y = \sum\frac{C_p n_y \Delta A}{S_{ref}} \tag{9}$$

$$C_z = \sum\frac{C_p n_z \Delta A}{S_{ref}} \tag{10}$$

Thus, based on the impact angle and the incoming flow conditions, each aerodynamic parameter of the vehicle can be calculated.

Lift factor:

$$C_L = -C_x \sin\alpha + C_z \cos\alpha \tag{11}$$

Non-viscous drag coefficient:

$$C_D = C_x \cos\alpha \sin\beta + C_y \sin\beta + C_z \sin\alpha \cos\beta \tag{12}$$

Pitch moment coefficient:

$$C_M = \frac{\left[\sum C_p\left(x - x_{CG}\right)n_z\Delta A - \sum C_p\left(z - z_{CG}\right)n_x\Delta A\right]}{\left(S_{ref}b_{ref}\right)} \tag{13}$$

S_{ref} is the reference surface area of the vehicle, b_{ref} is Feature-length, and CG is the position of the center of gravity.

3. Using the Template

The measured flow field at the windward surface of the NASA Space Shuttle STS Columbia OV-102 is provided in Ref. 2. A program was used to calculate the surface pressure coefficients at the streamlines along the center streamline of the Shuttle orbiter, and the flow chart of the space shuttle is divided by tecplot, as shown in Figure 2.

Using Solidworks to model the spacecraft STS Columbia OV-102, the program calculations were imported into the post-processing Tecplot software. The surface flow lines were divided using stream traces, as shown in Figure 3.

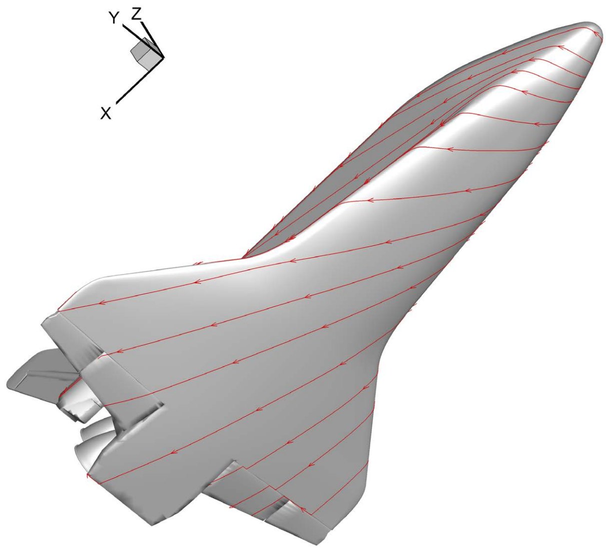

Figure 2. Calculated surface flow lines of the spacecraft based on Newton's most rapid descent theory.

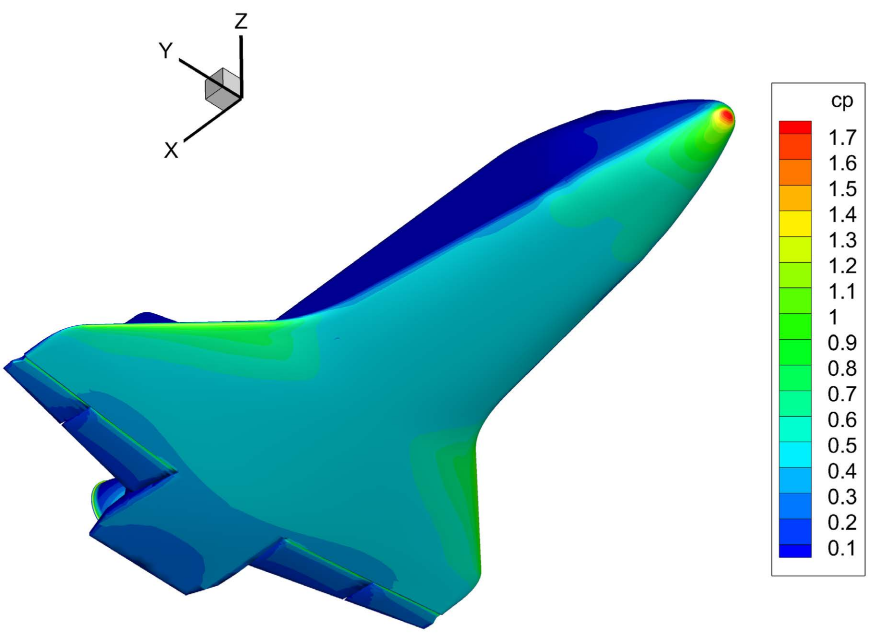

Figure 3. Surface pressure coefficient at 30˚ angle of attack for spacecraft.

Figure 4 compares the calculated and measured pressure coefficients for two angles of attack along Ma = 8 along the windward centerline, with L being the longitudinal length of the spacecraft [11]. The calculated pressure distribution obtained, although slightly higher, predicts the pressure in the middle region of the body, with an increase in the angle of attack and a slight shift of the beginning of the flow line a little bit from the center of the nose. However, it agrees with the experimental values in terms of distribution and horizontal results.

4. Program Calculation Results and Analysis

The HL-20 space shuttle orbiter model can be exported through the open-source open-vsp software to export the geometric model file, as shown in Figure 5(a).

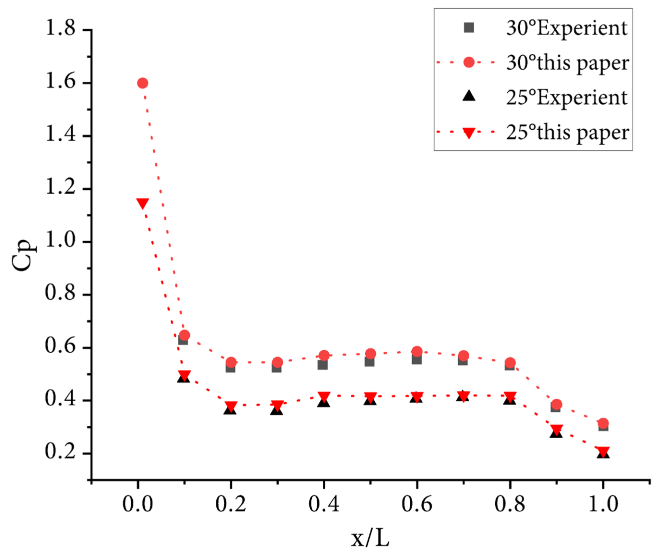

Figure 4. Comparison of pressure distribution on the windward centerline with experimental data.

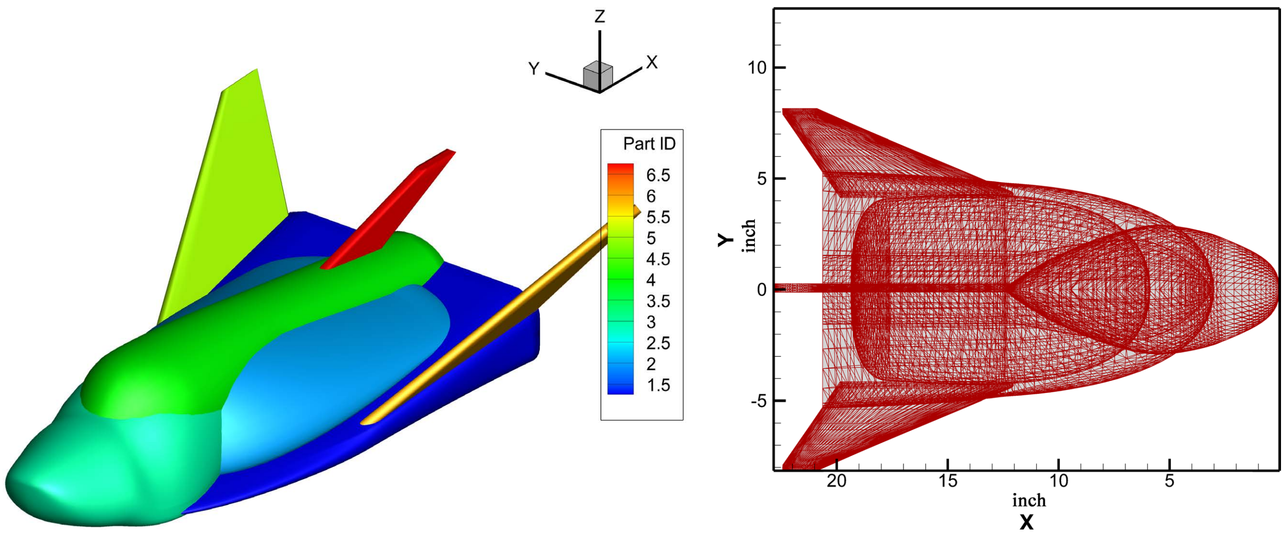

(a) (b)

Figure 5. HL-20 space orbiter model and STL format model.

The model is imported into the pre-processing software proe5.0 for meshing, as shown in Figure 5(b).

In NASA wind tunnel experiments, a large amount of experimental data is provided in the experimental environment from negative to positive angles of attack (−5˚ to 35˚) at speeds from Mach 1.5 to Mach 10. In this paper, the aerodynamic characteristics data at different angles of attack are selected for arithmetic verification under the operating conditions of Ma = 6 and 10. The calculated results are compared with the wind tunnel experimental data for analysis.

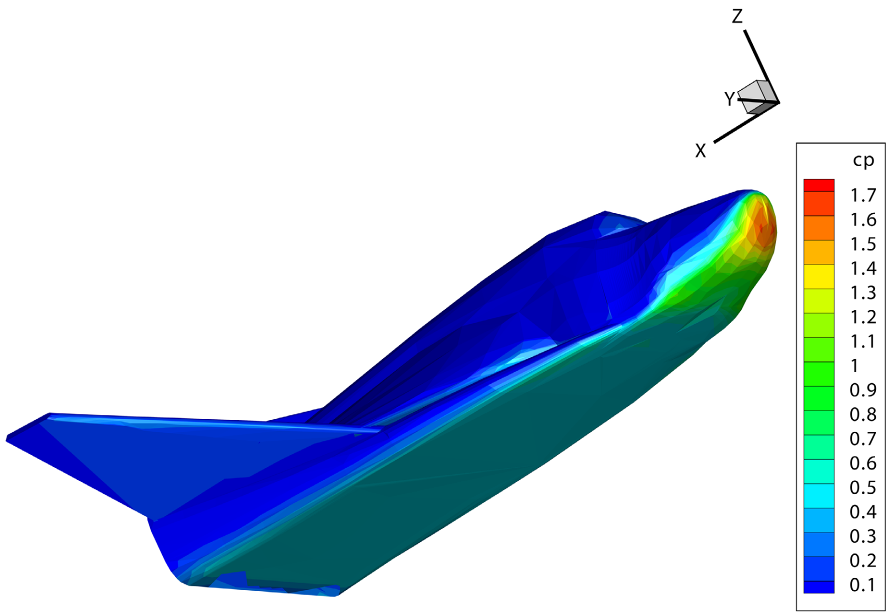

Figure 6. HL-20 lift body 30˚ angle of attack surface pressure coefficient.

4.1. HL-20 Aerodynamic Characteristics Program Calculation at Ma = 6

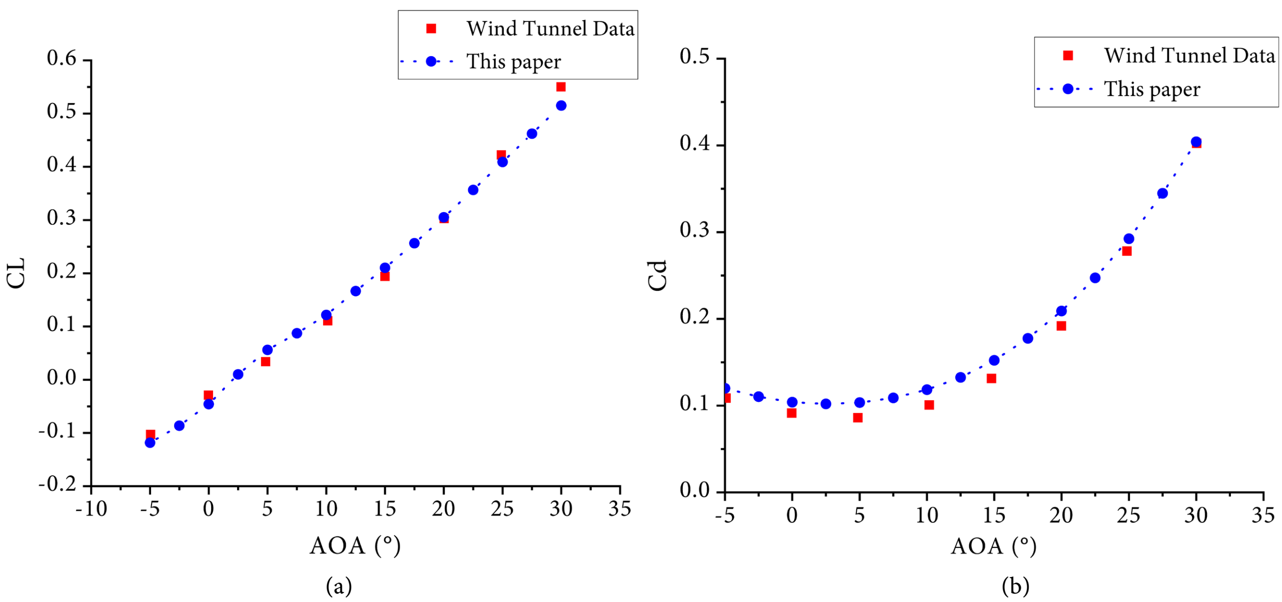

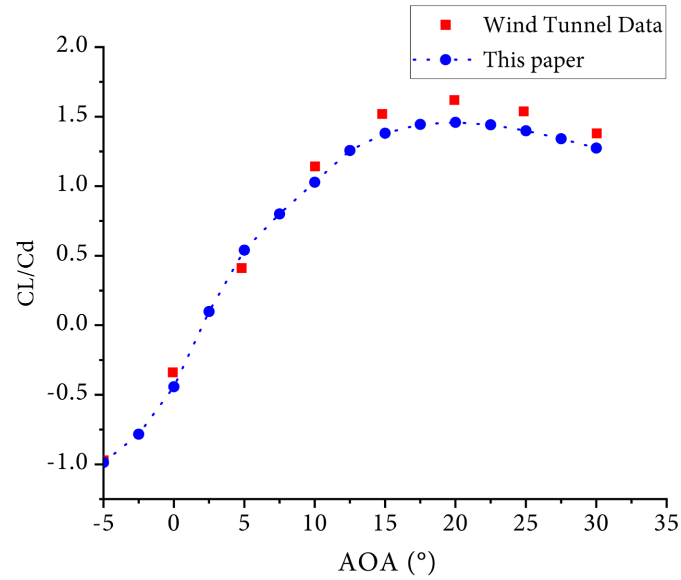

(c)

Figure 7. Comparison of HL-20 Mach number 6 surface pressure coefficient values with the angle of attack and wind tunnel values. (a) Lift coefficient at Mach 6; (b) Drag coefficient at Mach 6; (c) Lift to resistance ratio at Mach 6

4.2. HL-20 Aerodynamic Characteristics Program Calculation at Ma = 10

As shown in Figures 6-8, Figure 6 shows the distribution of surface pressure coefficient of the lift body model at 6 Ma and 30˚ angle of attack, which is consistent with the distribution of pressure coefficient at a large angle of attack; Figure 7 and Figure 8 show the changes in aerodynamic characteristics of the HL-20 lift body with the angle of attack at 6 Ma and 10 Ma, respectively, and compare the calculated results of the program with the wind tunnel experimental data. At 6 Ma, the calculated results of the program are in good agreement

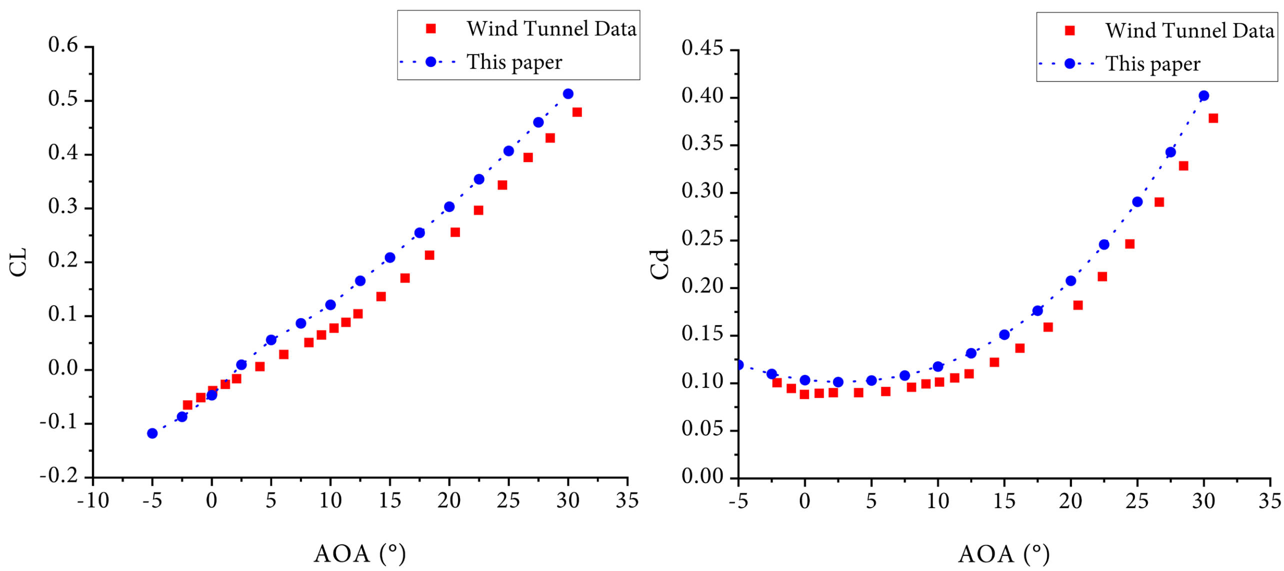

(a) (b)

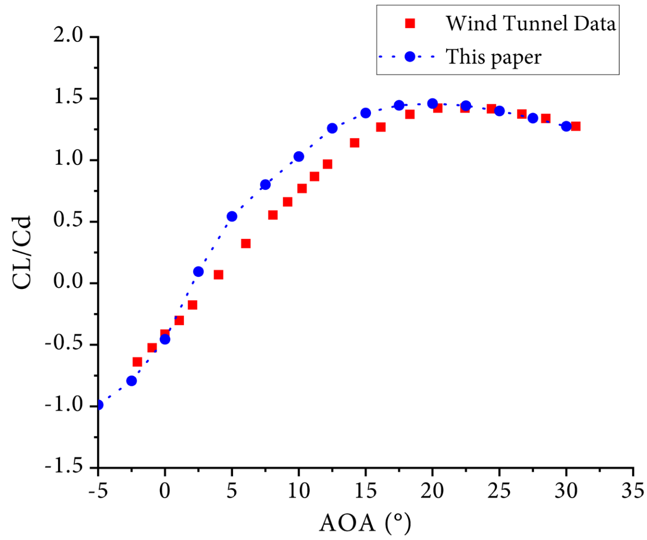

(c)

Figure 8. Comparison of HL-20 Mach number 6 surface pressure coefficient values with the angle of attack and wind tunnel values. (a) Lift coefficient at Mach 10; (b) Lift coefficient at Mach 10; (c) Lift to resistance ratio at Mach 10.

with the wind tunnel experimental values. At 10 Ma, with the increase of the angle of attack, the maximum error of the lift coefficient appears at the angle of attack of 20˚, the error is 16%, and the error of the drag coefficient is not more than 5%.

5. Conclusion

In this study, an STL surface mesh-based procedure is proposed for the aerodynamic prediction of hypersonic vehicles to calculate the aerodynamic properties of hypersonic velocities. Different Mach numbers, angles of attack, and models are used to calculate the surface pressure distribution. The surface pressure coefficients along the central axis of the STS Columbia OV-102 are calculated using the streamline tracking technique. The calculated results were verified with wind tunnel experimental data of the HL-20 high-lift body vehicle at Mach 6 and Mach 10, and the results were in good agreement. The variation of aerodynamic properties was obtained for the given conditions. An appropriate method of surface pressure calculation was chosen for this study. The results show that the method's accuracy is good due to selecting an appropriate surface pressure calculation method in each region of the hypersonic vehicle surface. The number of HL-20 high-lift surface elements is 43,587. Compared to the usual CFD calculations, the aerodynamic calculation program in this paper runs on an 11th generation Intel(R) Core(TM) i5-1135G7 processor in only 210 seconds of physical time. A set of 20 iterations from negative to positive angles of attack (−5˚ to 30˚) can be run in 0.5 hours. Based on the low time consumption of this method, the accuracy is high. It will be more versatile and flexible in the early design phase of hypersonic vehicles, especially in optimizing hypersonic vehicle configurations and surface hypersonic heat flow transport calculations. In future work, the results of the aerodynamic characteristic coefficients calculated by the procedure in this paper can be used in the Kemp-Riddell heat flow formulation for heat transfer coefficient and heat flow density calculations [12]. The results of hypersonic surface heat transfer coefficients and heat flux calculations based on wall parameters discuss the effect of Stanton number variations on heat transfer. The problem of large errors and long calculation time for hypersonic vehicles' aerodynamic and heat transfer simulations is solved.

Conflicts of Interest

The authors declare no conflicts of interest regarding the publication of this paper.

References

[1] Irimpan, K.J., Menezes, V., Srinivasan, K. and Hosseini, H. (2018) Nose-Tip Transition Control by Surface Roughness on a Hypersonic Sphere. *Journal of Flow Control, Measurement & Visualization,* **6**, 125-135. https://doi.org/10.4236/jfcmv.2018.63011

[2] Li, J., Jiang, D., Geng, X. and Chen, J. (2021) Kinetic Comparative Study on Aerodynamic Characteristics of Hypersonic Reentry Vehicle from Near-Continuous Flow to Free Molecular Flow. *Advances in Aerodynamics,* **3**, Article No. 10. https://doi.org/10.1186/s42774-021-00063-0

[3] Zhao, T., Ren, W., Yin, T. and Wang, F. (2021) Calculation of the Coupling Coefficient of Twin-Core Fiber Based on the Supermode Theory with Finite Element Method. *Optics and Photonics Journal,* **11**, 402-411. https://doi.org/10.4236/opj.2021.118029

[4] Ware, G.M. and Cruz, C.I. (1993) Aerodynamic Characteristics of the HL-20. *Journal of Spacecraft and Rockets,* **30**, 529-536. https://doi.org/10.2514/3.25562

[5] Yang, Z., Wang, S. and Gao, Z. (2022) Studies on Effects of Wall Temperature Variation on Heat Transfer in Hypersonic Laminar Boundary Layer. *International Journal of Heat and Mass Transfer,* **190**, Article ID: 122790. https://doi.org/10.1016/j.ijheatmasstransfer.2022.122790

[6] Yilmaz, Y. and Ozturan, C. (2015) Using Sequential NETGEN as a Component for a Parallel Mesh Generator. *Advances in Engineering Software,* **84**, 3-12. https://doi.org/10.1016/j.advengsoft.2014.12.013

[7] Schöberl, J. (2016) Netgen Mesh Generator. https://sourceforge.net/projects/netgen-mesher/

[8] Lyu, F.X., Li, Z.Z., Deng, J.S., Xiao, T.H. and Yu, X.Q. (2017) An Aerodynamic Analysis Tool for Aircraft Conceptual Design at Full Speed Range. *Acta Aerodynamica Sinica,* **35**, 625-632.

[9] Chang, X.H., Ma, R., Wang, N.H. and Zhang, L.P. (2018) Parallel Implicit Hole-Cutting Method for Unstructured Chimera Grid. *Acta Aeronautica et Astronautica Sinica,* **39**, 48-58.

[10] Zhao, M. (2021) Prediction and Validation Technologies of Aerodynamic Force and Heat for Hypersonic Vehicle Design. Springer Nature, Berlin. https://doi.org/10.1007/978-981-33-6526-1

[11] Martindale, W.R. and Carter, L.D. (1975) Flow-Field Measurements in the Wind-

ward Surface Shock Layer of Space Shuttle Orbiter Configurations at Mach Number 8. Arnold Engineering Development Center, Arnold Afb Tn. https://doi.org/10.21236/ADA012875

[12] Wang, P., Fang, S.A., Jin, X. and Zhang, W.M. (2017) Calculation Methods for Aerodynamic Thermal Characteristics of Aerospace Vehicles at Hypersonic Speeds. *Chinese Journal of Aerodynamics*, **35**, 640-644.